Intracellular pH-regulating Mechanism of the Squid Axon

Relation Between the External Na^+ and HCO_3^- Dependences

WALTER F. BORON

From the Department of Physiology, Yale University School of Medicine, New Haven, Connecticut 06510

ABSTRACT The intracellular pH–regulating mechanism of the squid axon was examined for its dependence on the concentrations of external Na^+ and HCO_3^-, always at an external pH (pH_o) of 8.0. Axons having an initial intracellular pH (pH_i) of ~7.4 were internally dialyzed with a solution of pH 6.5 that contained 400 mM Cl^- and no Na^+. After pH_i had fallen to ~6.6, dialysis was halted, thereby returning control of pH_i to the axon. With external Na^+ and HCO_3^- present, intracellular pH (pH_i) increased because of the activity of the pH_i-regulating system. The acid extrusion rate (i.e., equivalent efflux of H^+, J_H) is the product of the pH_i recovery rate, intracellular buffering power, and the volume-to-surface ratio. The $[HCO_3^-]_o$ dependence of J_H was examined at three fixed levels of $[Na^+]_o$: 425, 212, and 106 mM. In all three cases, the apparent J_{max} was ~19 pmol·cm^{-2}·s^{-1}. However, the apparent K_m (HCO_3^-) was approximately inversely proportional to $[Na^+]_o$, rising from 2.6 to 5.4 to 9.7 mM as $[Na^+]_o$ was lowered from 425 to 212 to 106 mM, respectively. The $[Na^+]_o$ dependence of J_H was similarly examined at three fixed levels of $[HCO_3^-]_o$: 12, 6, and 3 mM. The J_{max} values did not vary significantly from those in the first series of experiments. The apparent K_m (Na^+), however, was approximately inversely related to $[HCO_3^-]_o$, rising from 71 to 174 to 261 mM as $[HCO_3^-]_o$ was lowered from 12 to 6 to 3 mM, respectively. These results agree with the predictions of the ion-pair model of acid extrusion, which has external Na^+ and $CO_3^=$ combining to form the ion pair $NaCO_3^-$, which then exchanges for internal Cl^-. When the J_H data are replotted as a function of $[NaCO_3^-]_o$, data from all six groups of experiments fall along the same Michaelis-Menten curve, with an apparent K_m ($NaCO_3^-$) of 80 μM. The ordered and random binding of Na^+ and $CO_3^=$ cannot be ruled out as possible models, but are restricted in allowable combinations of rate constants.

J. GEN. PHYSIOL. © The Rockefeller University Press · 0022-1295/85/03/0325/21 $1.00 325
Volume 85 March 1985 325–345

INTRODUCTION

The intracellular pH (pH_i) of the squid giant axon is regulated by a mechanism, located in the cell membrane, that mediates the uptake of both Na^+ and HCO_3^- (or a related ion) and the efflux of Cl^- and possibly H^+. This mechanism responds to decreases in pH_i by increasing its rate of transport (i.e., acid extrusion). Its stoichiometry is one mole of Na^+ taken up for each mole of Cl^- lost and for every two equivalents of acid neutralized inside the cell (Boron and Russell, 1983). Fig. 1 illustrates four models that can account for this stoichiometry. The

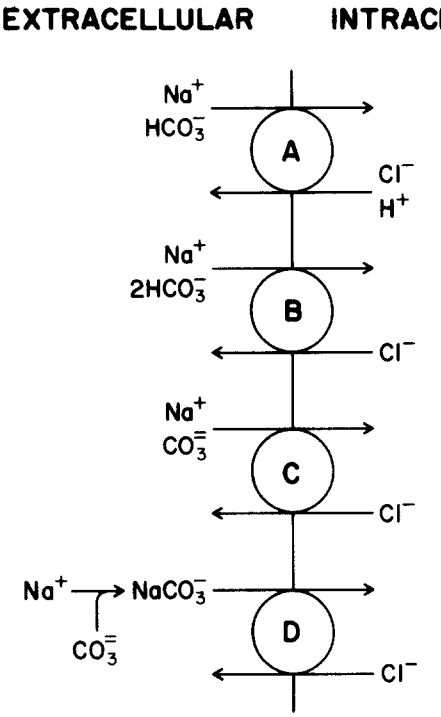

FIGURE 1. Models of acid extrusion. (*A*) External Na^+ plus HCO_3^- exchange for Cl^- plus H^+ (Thomas, 1977). (*B*) The entry of a second HCO_3^- replaces the exit of H^+. (*C*) The entry of a single $CO_3^=$ is equivalent to that of the two HCO_3^- above. (*D*) $CO_3^=$ ($CO_3^= = H^+ + HCO_3^-$) combines with Na^+ to form the ion pair $NaCO_3^-$, the entry of which is equivalent to the separate influx of Na^+ and $CO_3^=$ in *C* above.

first (Fig. 1*A*) has Na^+ and HCO_3^- exchanging for Cl^- plus H^+ (Thomas, 1977). In the second (Fig. 1*B*), the exit of H^+ is replaced by the entry of a second HCO_3^-. In the third model (Fig. 1*C*), the entry of two HCO_3^- is replaced by that of a single $CO_3^=$. Finally, in the fourth model (Fig. 1*D*), the separate entry of Na^+ and $CO_3^=$ is replaced by the entry of a single $NaCO_3^-$ ion pair (Becker and Duhm, 1978). Although these four models are equivalent thermodynamically, they do not necessarily lead to identical kinetic predictions. In particular, the ion-pair model requires that the acid extrusion rate (J_H) be a unique function of neither

extracellular $[Na^+]$ ($[Na^+]_o$) or $[HCO_3^-]_o$, but rather of $[NaCO_3^-]_o$. At a fixed pH_o, $[NaCO_3^-]_o$ is proportional to the product $[Na^+]_o \cdot [HCO_3^-]_o$.

pH_i-regulating mechanisms qualitatively similar to the squid axon's have been described in snail neurons (Thomas, 1977), crayfish neurons (Moody, 1981), and barnacle muscle (Boron et al., 1981). In particular, the transporters in all four preparations are blocked by 4-acetamido-4′-isothiocyano-2,2′-disulfonate (SITS), and involve internal Cl^- as well as external Na^+ and HCO_3^-. Kinetic analyses are limited to the squid axon (Boron and Russell, 1983) and barnacle muscle (Boron et al., 1981). In both preparations, Michaelis-Menten kinetics adequately describe the dependence of J_H on $[Na^+]_o$ at a single $[HCO_3^-]_o$ (12 and 10 mM, respectively, for squid and barnacle), as well as the dependence of J_H on $[HCO_3^-]_o$ at a single $[Na^+]_o$ (425 and 440 mM). The ion-pair model requires that plotting these J_H data as a function of the calculated $[NaCO_3^-]_o$ should cause all the data to fall along the same J_H vs. $[NaCO_3^-]_o$ curve, regardless of whether $[Na^+]_o$ was varied at a single $[HCO_3^-]_o$ or vice versa. The aforementioned data fulfill this prediction for both squid axons and barnacle muscle. However, when the barnacle study was extended to include the dependence of J_H on $[Na^+]_o$ at a second fixed level of $[HCO_3^-]_o$ (i.e., 2.5 mM), the additional data fell on a J_H vs. $[NaCO_3^-]_o$ curve very different from the first. Thus, taken together, the J_H vs. $[Na^+]_o$ data at 2.5 and 10 mM HCO_3^- allow us to rule out the ion-pair model for barnacle muscle. The question that arises is whether a more extensive kinetic analysis on the squid axon would produce data that are also inconsistent with the ion-pair model. Given several other minor differences between the pH_i-regulating systems of barnacle muscle and squid axons (see Discussion), I felt the likelihood of substantial kinetic discrepancies to be significant.

In the present work, I examine J_H as a function of $[Na^+]_o$ at three fixed levels of $[HCO_3^-]_o$, and as a function of $[HCO_3^-]_o$ at three fixed levels of $[Na^+]_o$. The present study is more complete than the earlier one on barnacle (Boron et al., 1981), in which Na^+ dependence was examined at only two $[HCO_3^-]_o$ values and HCO_3^- dependence was examined at only one $[Na^+]_o$. Furthermore, whereas the previous kinetic studies on either barnacle or squid were performed on intact cells, the present study was performed on internally dialyzed axons. This permitted tight control of the intracellular environment with respect to Na^+ and Cl^-, and thus it had two theoretical advantages over the earlier kinetic studies: (*a*) because the dialysate was Na^+ free, the reverse reaction, in which Na^+ plus HCO_3^- (or an equivalent species) could leave the cell, was obviated; (*b*) because $[Cl^-]$ was very high in the dialysate, the transporter was nearly saturated with respect to internal Cl^-. I found that all of the present data fall along a single J_H vs. $[NaCO_3^-]_o$ curve. The results are thus consistent with the ion-pair model and place restrictions on other kinetic models.

METHODS

General

The experiments were conducted at the Marine Biological Laboratory, Woods Hole, MA, during May and June, 1983. Live specimens of the squid *Loligo pealei* were decapitated, and the first stellar nerve from each side was removed and placed in cold Woods Hole

seawater. A 4–5-cm length of giant axon (generally 400–600 μm in diameter) was isolated from the nerve by microdissection, cannulated at both ends, and mounted horizontally in a chamber (see Boron and Russell, 1983) designed for internal dialysis (Brinley and Mullins, 1967). A length of dialysis tubing (see below) was threaded through one cannula, down the length of the axon, and out the opposite cannula. In addition, pH- and voltage-sensitive microelectrodes were introduced through opposite cannulas, so that their tips were within 500 μm of each other at the middle of the axon. Artificial seawater continuously flowed around the axon. The temperature, controlled by a circulating water bath connected to the water jacket on the underside of the chamber, was 22°C.

Solutions

The standard external fluid (i.e., squid seawater [SSW]) had the following composition (in mM): 425.2 Na^+, 12 K^+, 3 Ca^{++}, 57.5 Mg^{++}, 531 Cl^-, 12 HCO_3^-, 0.1 $EDTA^=$, 15 of the anionic form of [2-hydroxyethyl]-1-piperazine-propane sulfonic acid (EPPS), and 15 of the neutral form of EPPS (pK ~8.0). The pH was 8.00, and the osmolality was ~980 mosmol. In experiments in which $[Na^+]_o$ was lowered, the Na^+ was replaced mole for mole by *N*-methyl-D-glucammonium, the latter made by titrating the free base (Sigma Chemical Co., St. Louis, MO) with HCl. When $[HCO_3^-]_o$ was varied, HCO_3^- was exchanged for Cl^- on a mole-for-mole basis.

The HCO_3^--containing seawaters were made as follows. All components except HCO_3^- (added as the K^+ or Na^+ salt) were combined and brought to 99% of the final volume, and then titrated to pH 8.00 with HCl or *N*-methyl-D-glucamine. For solutions having an $[HCO_3^-]$ of ≤12 mM, $KHCO_3$ was then added from a 1.21-M stock solution. HCO_3^--containing SSWs having a $[HCO_3^-]$ of 24 or 48 mM were made similarly, except that the HCO_3^- was added as powdered $NaHCO_3$. The addition of HCO_3^- caused the pH to decrease anomalously (by ~0.03 in the case of 12 mM HCO_3^-), probably because more of the added HCO_3^- underwent the reaction $HCO_3^- \rightarrow H^+ + CO_3^=$ than underwent the alternative reaction sequence $HCO_3^- + H^+ \rightarrow H_2CO_3 \rightarrow H_2O + CO_2$. The pH was returned to 8.00 by briefly gassing the solution with 100% O_2 while vigorously stirring. Inasmuch as the CO_2 evolution procedure required a few minutes, there is little doubt that the CO_2 dehydration reaction (time constant at room temperature, ~0.04 s) was allowed sufficient time to go to completion. Because ~1% of the added HCO_3^- goes on to form $CO_3^=$ and another ~1% goes on to form CO_2, the actual $[HCO_3^-]$ is at least ~2% lower than the nominal value. In addition, the CO_2 evolution procedure for returning the pH to 8.00 probably causes the loss of another ~4% of HCO_3^- at a nominal $[HCO_3^-]$ of 48 mM, ~2.5% at a nominal $[HCO_3^-]$ of 12 mM, and correspondingly smaller losses at lower nominal HCO_3^- concentrations. The SSW was drawn up into 140-ml plastic syringes, which were then capped. Such solutions can be stored in the refrigerator for at least 18 h and still maintain the proper pH and (by bioassay) pCO_2. The advantage of making HCO_3^--containing solutions in this way is that the technique obviates the need for expensive gas mixtures. HCO_3^--containing SSWs were delivered to the chamber via CO_2-impermeable Saran tubing (Clarkson Equipment and Controls, Detroit, MI).

In the initial and final phases of each experiment, the axons were exposed to HCO_3^--free SSW. This was the same as standard SSW except that it contained only 10 mM K^+, was HCO_3^--free (Cl^- replacing HCO_3^-), and for purposes of economy contained only 10 mM total EPPS ($MgCl_2$ replacing MgEPPS on an osmole-for-osmole basis).

The internal dialysis fluid (DF) had the following composition (in mM): 0 Na^+, 415.3 K^+, 7 Mg^{++}, 8 Tris, 400 Cl^-, 14 glutamate, 4 $ATP^=$, 1 $EGTA^=$, 13.3 of the anionic form of 2-[*N*-morpholino]-ethanesulfonic acid (MES), 6.7 of the neutral form of MES, 215 glycine, and 0.5 phenol red. The pH was adjusted to 6.50 with HCl or KOH, and the

osmolality was adjusted to ~980 mosmol with glycine. The ATP was added to the DF on the day of the experiment from a 400-mM (pH 7.0) stock solution stored at −5°C.

Internal Dialysis

The internal dialysis technique (Brinley and Mullins, 1967) permits control of the intracellular ionic environment. Details of my use of the method can be found in an earlier paper (Boron and Russell, 1983). The dialysis capillaries (140 μm o.d.) were made of cellulose acetate tubing (Fisher Research Laboratories, FRL, Inc., Dedham, MA), an 18-mm-long portion of which was rendered porous to low-molecular-weight solutes by soaking it in 0.1 N NaOH for 18–24 h. The central region of the axon, which was dialyzed and in which the tips of the pH- and voltage-sensitive electrodes resided, was isolated from the cannulated ends of the axon by grease seals (a mixture of vaseline and mineral oil). The dialysis capillary was perfused with DF at the rate of ~5 μl/min.

Measurement of pH_i

As noted above, pH- and voltage-sensitive electrodes were introduced through opposite cannulas, alongside the dialysis capillary. The pH-sensitive electrodes were of the design of Hinke (1967), fabricated of lead glass (0120, Corning Glass Works, Corning, NY) and pH-sensitive glass (Clark Electromedical Instruments, Pangbourne, England). The lead glass shank had an outer diameter of <125 μm for at least the terminal 3 cm. The pH-sensitive tips had outer diameters of ~50 μm at the glass-glass seal and exposed lengths of 200–300 μm. The electrodes were filled with 0.1 M HCl and fitted with Ag/AgCl half-cells. They were calibrated in high-ionic-strength buffers (Boron and De Weer, 1976). The voltage-sensitive electrodes were similar to the pH electrodes, but had open tips (~10 μm diam), were filled with 0.5 M KCl, and were fitted with a calomel half-cell. A second calomel half-cell, the tip of which was placed directly in the SSW exit port, served as the external reference electrode. The system was grounded via a platinum/iridium wire placed in the chamber. The signals from the pH- and voltage-sensitive electrodes were amplified by separate channels of a high-impedance (10^{15} Ω) electrometer (model 223, W-P Instruments, Inc., New Haven, CT), and the signal from the external reference electrode was amplified by one channel of an electrode amplifier (10^{11} Ω input impedance, model M750, W-P Instruments, Inc.). The electronically obtained difference between the signals from the pH- and voltage-sensitive electrodes is the voltage due solely to pH_i, and was plotted by a strip-chart recorder and sampled every 10 s by an analog-to-digital converter (AD-212, Tekmar Co., Cinncinnati, OH) interfaced to a Horizon computer (Northstar, San Leandro, CA). The difference between the signals from the voltage-sensitive and external reference electrodes represents membrane potential (V_m) and was processed similarly.

Calculation of Acid Extrusion Rates

I define the acid extrusion rate (J_H) as the flux (if any) of H^+ out of the cell plus the flux of HCO_3^- (or a related species) into the cell. My approach was to acid load axons by dialyzing with a pH 6.5 solution, and to halt dialysis when pH_i reached ~6.6. The pH_i-regulating system then extrudes acid from the cell (provided Na^+ and HCO_3^- are present in the external solution), causing pH_i to rise. J_H is the product of the rate of pH_i recovery (dpH_i/dt) from the imposed acid load, the axon's volume-to-surface ratio, and the total intracellular buffering power (β_T). dpH_i/dt was usually determined by a linear least-squares fit of the pH_i recovery data, previously acquired by the computer. However, the computer was nonfunctional for approximately the first 30% of the experiments and malfunctioned in some of the others. For these experiments, dpH_i/dt was determined by

drawing a line through a strip-chart recording of the data. The volume-to-surface ratio is one-fourth of the axon's diameter, assuming the axon to be a cylinder. β_T is the sum of the intrinsic or non–CO_2-buffering power (β_I) and the CO_2-buffering power (β_{CO_2}). In a previous study (Boron and Russell, 1983), it was found that the empirically determined β_I did not differ significantly from the calculated buffering power of the DF used in that study. Accordingly, I have assumed that in the present study β_I is 11.2 mM, the buffering power calculated for the present DF. β_{CO_2} was individually calculated for each segment of pH_i recovery. In a system in which CO_2 can freely equilibrate with the environment, $\beta_{CO_2} = (\ln 10)\,[HCO_3^-]$. $[HCO_3^-]_i$ was calculated from pH_i, assuming equal CO_2 tensions inside and outside the axon, taking as pH_i the value at the midpoint of the interval used to obtain dpH_i/dt.

Curve-fitting Procedures

The acid extrusion rate data were fitted to the Michaelis-Menten equation using nonlinear least-squares methods (Scarborough, 1966). The equation is of the form $J_H = s \cdot J_{max}/(s + K_m)$, where s is substrate concentration, J_{max} is the apparent maximal J_H, and K_m is the apparent Michaelis constant. Three types of fits were performed. For a type 1 fit, the data were fitted to the standard Michaelis-Menten equation, resulting in best-fit values for both K_m and J_{max}. For a type 2 fit, the curve was forced through an arbitrary point, in addition to the origin. As described in the Results, for each axon I determined J_H in a "standard" solution having $[Na^+]_o$ = 425 mM and $[HCO_3^-]_o$ = 12 mM, and in three additional "test" combinations of $[Na^+]_o$ and $[HCO_3^-]_o$. To reduce scatter, I analyzed the data as the ratio J_H(test)/J_H(standard), not as absolute fluxes. In the analysis of the dependence of J_H on $[Na^+]_o$ at a fixed $[HCO_3^-]_o$ of 12 mM, there were no independently determined values for the J_H(test)/J_H(standard) ratio at a $[Na^+]_o$ of 425 mM, even though, by definition, this ratio must be unity. A similar situation existed for the analysis of the dependence of J_H on $[HCO_3^-]_o$ at a fixed $[Na^+]_o$ of 425 mM, in which case the ratio J_H(test)/J_H(standard) was not determined independently at an $[HCO_3^-]_o$ of 12 mM. The following variant of the Michaelis-Menten equation forces the curve through the standard point, having coordinates $s = s'$ and $J_H = J'$:

$$J = sJ'(s' + K_m)/[s'(s + K_m)].$$

K_m is estimated from a nonlinear least-squares fit, and J_{max} is then calculated from this K_m, according to the equation $J_{max} = (s' + K_m)J'/s'$. A type 3 fit treats the Michaelis-Menten equation as having only one fittable parameter, K_m. J_{max} is assumed to be independently known. This type of fit was used in the provisional analysis of data for which the concentration of substrate (i.e., Na^+) could not be raised sufficiently above the expected K_m to allow an optimal curve-fit determination of J_{max} and K_m.

Switching of Solutions

The computer not only acquired the data, but also executed the solution changes. The syringe drivers that delivered the CO_2-containing SSWs (model 975, Harvard Apparatus Co., Inc., South Natick, MA) and the syringe driver that delivered the DF (model 341A, Sage Instruments Div., Cambridge, MA) were switched on and off by computer-controlled relays into which their line cords were plugged. The peristaltic pump that delivered the CO_2-free SSW (model 2132, LKB Instruments, Inc., Gaithersburg, MD) was also controlled by a computer-activated relay. The inputs and outputs of four four-way Kel-F/Teflon values (model 201-05, Altex Scientific Inc., Berkeley, CA) were chained together, so that the valve assembly had one output to the dialysis chamber and five inputs (one from the CO_2-free SSW and four from CO_2-containing SSWs). The Altex valves were

switched by pneumatic pistons, which in turn were activated by computer-controlled switches. Because the experimental protocol was standard, the computer could be programmed to decide when to switch solutions, based on pH_i, dpH_i/dt, and the elapsed time in a given solution.

Statistics

The K_m and J_{max} values, derived from nonlinear least-squares curve fits, are given ± the standard deviation. Mean values of acid extrusion rates and intracellular pH are given ± the standard error.

RESULTS

Experimental Protocol

Acid-extruding transport systems in intact cells are best studied by acutely acid loading the cell and monitoring the subsequent recovery of pH_i. In the present experiments, the acid loading was accomplished by dialyzing the axon with a dialysis fluid (DF) having a nominal pH of 6.5. Because the DF was also Na-free, the possible reversal of the transporter was prevented. In addition, the DF contained 400 mM Cl^-. Inasmuch as a previous study (Boron and Russell, 1983) had shown that the apparent K_m for internal Cl^- is ~84 mM, 400 mM Cl^- should have left the transporter ~83% saturated with respect to Cl^-, provided the K_m is not influenced by lowering $[Na^+]_i$. A typical experiment is illustrated in Fig. 2. Initiation of dialysis (point *a*) causes a rapid acidification of the axoplasm. From an initial value of ~7.5, pH_i reaches 6.7 after ~45 min. pH_i probably would have approached ~6.6 had dialysis been continued for a longer period. Previous work with Na^+ and Cl^- isotopic fluxes (Boron and Russell, 1983), as well as more recent data obtained with Cl^--sensitive microelectrodes (J. M. Russell, personal communication), indicate that 45 min of dialysis is sufficient for $[Na^+]_i$ and $[Cl^-]_i$ to closely approach their levels in the DF. After dialysis is halted (*b*), pH_i increases by 0.01 and then is relatively stable. This time of relative stability just before point *c* is the initial baseline period referred to below. When the external fluid is switched from HCO_3^--free SSW to SSW containing 425 mM Na^+ and 12 mM HCO_3^- at pH 8.00, there is a slight decrease in pH_i (segment *cd*) caused by the influx of CO_2, which is followed by a rapid increase of pH_i (*de*). The pH_i recovery shown by segment *de* is due to acid extrusion by the pH_i-regulating system and corresponds to an acid extrusion rate (J_H) of 20.8 pmol·cm^{-2}·s^{-1}. The subsequent reduction of $[Na^+]_o$ to 26.5 mM at constant $[HCO_3^-]_o$ (*ef*) slows the pH_i recovery to a rate corresponding to a J_H of 9.4 pmol·cm^{-2}·s^{-1}. At point *f*, $[HCO_3^-]_o$ and pCO_2 are simultaneously reduced to one-fourth of their initial values at constant pH_o (8.00) and $[Na^+]_o$ (26.5 mM). The reduction of pCO_2 causes a rapid rise of pH_i because of the efflux of CO_2 (*fg*), after which acid extrusion causes pH_i to rise at a very low rate (*gh*). dpH_i/dt in this segment corresponds to a J_H of only 0.9 pmol·cm^{-2}·s^{-1}. Raising $[Na^+]_o$ to 53 mM at constant $[HCO_3^-]_o$ causes the pH_i recovery rate to increase (*hi*) to a level consistent with a J_H of 4.1 pmol·cm^{-2}·s^{-1}. Finally, when the CO_2/HCO_3^- SSW is replaced by HCO_3^--free SSW, there is a rapid increase of pH_i caused by the efflux of CO_2

(*ij*), followed by a relative stabilization of pH_i during the final baseline period (*jk*).

The assumption that J_H is proportional to dpH_i/dt is valid only when all pH_i changes are due to the pH_i-regulating system. However, slight drifts in the pH_i

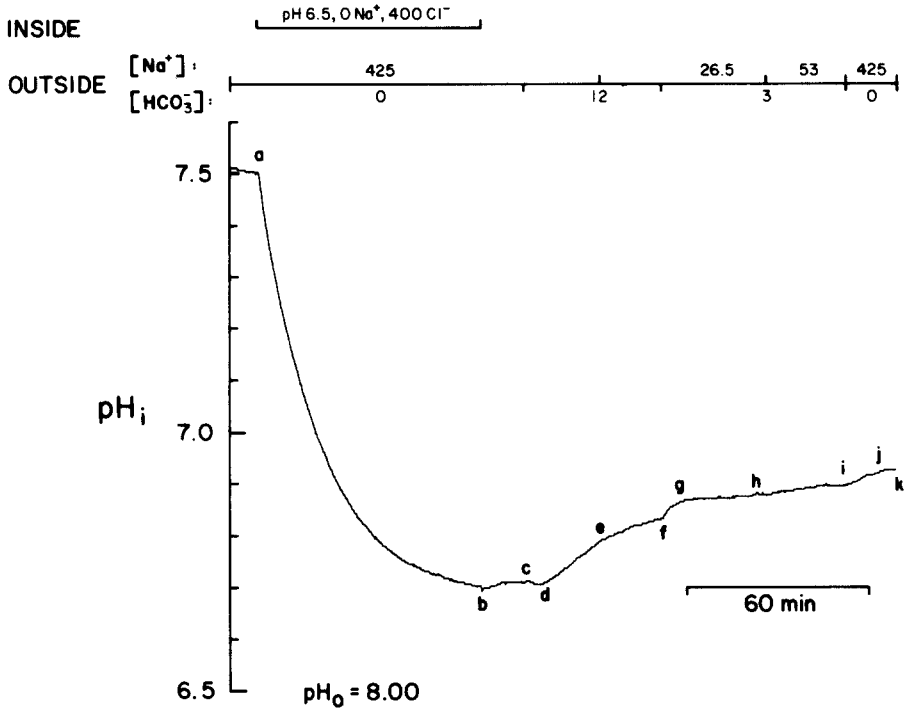

FIGURE 2. Effect on acid extrusion rate of altering $[Na^+]_o$ and/or $[HCO_3^-]_o$. At point *a*, the flow of dialysis fluid (DF) was begun, leading to a gradual fall of intracellular pH (pH_i). Because $[Na^+]_{DF} = 0$ and $[Cl^-]_{DF} = 400$ mM, the axoplasm also became low in Na^+ and high in Cl^-. At point *b*, dialysis was halted, so that the subsequent course of pH_i was determined by the axon. After a slight rise, pH_i stabilized at *c* (the initial baseline), failing to recover in the absence of HCO_3^-. The introduction of 12 mM HCO_3^- at *c* ($[Na^+]_o = 425$ mM) caused a rapid alkalinization (*de*). The pH_i recovery was slowed by lowering $[Na^+]_o$ to 26.5 mM (*ef*) while holding $[HCO_3^-]_o$ constant at 12 mM, and slowed even further by lowering $[HCO_3^-]_o$ to 3 mM while holding $[Na^+]_o$ constant at 26.5 mM (*gh*). Finally, doubling $[Na^+]_o$ to 53 mM while holding $[HCO_3^-]_o$ constant at 3 mM increased the rate of pH_i recovery (*hi*). The rapid acidification during *cd* was caused by the increase in pCO_2, whereas the rapid alkalinizations during *fg* and *ij* were due to decreasing pCO_2. pH_o was 8.00 throughout.

baseline often occur before the CO_2/HCO_3^- is introduced and/or after it is removed, and indicate that background acid or alkali loading may be influencing the calculated acid extrusion rates. Estimates of these background rates were subtracted from the gross J_H values as follows. I first performed a linear fit of

the pH_i time course in the initial (the region before *c*) and final baseline periods (segment *jk*). The slopes of these lines were then converted to initial and final background acid fluxes. The background flux, which was assumed to vary linearly between the initial and final baseline periods, was then subtracted from the total calculated flux during the periods of acid extrusion (i.e., from points *d* through *i*).

Because fluxes can vary considerably from axon to axon, I normalized the data in the following manner. For each axon, a J_H value was obtained under "standard" conditions of 425 mM Na^+/12 mM HCO_3^- (e.g., *de* in Fig. 2) and in up to three other "test" solutions (e.g., *ef*, *gh*, and *hi*). Each test J_H was expressed as a fraction of the standard J_H for that axon. After the data analyses were complete, the ratios were converted back into fluxes by multiplying them by the mean J_H in the standard solution, 15.3 ± 0.6 pmol·cm^{-2}·s^{-1} (n = 63 axons). As expected, this standard J_H is considerably higher than the value of 9.5 pmol·cm^{-2}·s^{-1} obtained previously (Boron and Russell, 1983) on intact (i.e., undialyzed) axons, for which $[Cl^-]_i$ was much lower, probably on the order of 100 mM (Brinley and Mullins, 1965; Russell, 1976).

Dependence of J_H on $[HCO_3^-]_o$

I determined the dependence of J_H on $[HCO_3^-]_o$ at three fixed levels of $[Na^+]_o$: 425, 212, and 106 mM. The results are plotted in Fig. 3 and summarized in Table I. The J_H data obtained in 425 mM Na^+ were fitted to a modified Michaelis-Menten equation (type 2 fit; see Methods) that forced the curve through the mean standard flux (i.e., 15.3 pmol·cm^{-2}·s^{-1}) under standard conditions (i.e., $[HCO_3^-]_o$ = 12 mM, $[Na^+]_o$ = 425 mM). This point is denoted by an asterisk in the figure. The K_m (HCO_3^-) in 425 mM Na^+ was 2.6 ± 0.3 mM, which is very similar to the value of 2.3 mM previously found for intact axons (Boron and Russell, 1983). This similarity suggests that the combination of raising $[Cl^-]_i$ from ~100 to 400 mM and reducing $[Na^+]_i$ to ~0 mM has little effect on K_m (HCO_3^-). J_{max} in these experiments was 18.6 ± 2.1 pmol·cm^{-2}·s^{-1}, considerably higher than the value of 10.6 pmol·cm^{-2}·s^{-1} obtained previously. As noted above, this discrepancy is probably due to the much higher $[Cl^-]_i$ in the present study. Indeed, in earlier work on dialyzed axons (Boron and Russell, 1983), in which $[Cl^-]_i$ was varied at a fixed $[Na^+]_o$ of 425 mM and a fixed $[HCO_3^-]_o$ of 12 mM, the J_{max} was 19.6 ± 1.2 pmol·cm^{-2}·s^{-1}. This is not significantly different from the value obtained in the present study, in which $[HCO_3^-]_o$ was varied at high $[Cl^-]_i$.

The data at $[Na^+]_o$ values of 212 and 106 mM were fitted to an unmodified Michaelis-Menten equation (type 1 fit; see Methods). When $[Na^+]_o$ was reduced by half, to 212 mM, K_m (HCO_3^-) approximately doubled, to 5.4 ± 1.0 mM. J_{max}, however, was 18.7 ± 1.2 pmol·cm^{-2}·s^{-1}, which is not significantly different from the value in 425 mM Na^+. Reducing $[Na^+]_o$ to one-fourth of its control value, to 106 mM, caused K_m (HCO_3^-) to increase by a factor of >3.7, to 9.7 ± 2.1 mM. Once again, J_{max} (19.2 ± 1.5 pmol·cm^{-2}·s^{-1}) was not significantly altered by the reduction of $[Na^+]_o$. The three K_m (HCO_3^-) values of Table I are all significantly different from one another ($P < 0.001$).

Dependence of J_H on $[Na^+]_o$

I examined the dependence of the acid extrusion rate on $[Na^+]_o$ at three different levels of $[HCO_3^-]_o$: 12, 6, and 3 mM. The results are plotted in Fig. 4 and summarized in Table II. The data at an $[HCO_3^-]_o$ of 12 mM were fitted to a modified Michaelis-Menten equation (type 1 fit), which forced the curve through the mean standard J_H (i.e., 15.3 pmol·cm^{-2}·s^{-1}) under standard conditions (i.e.,

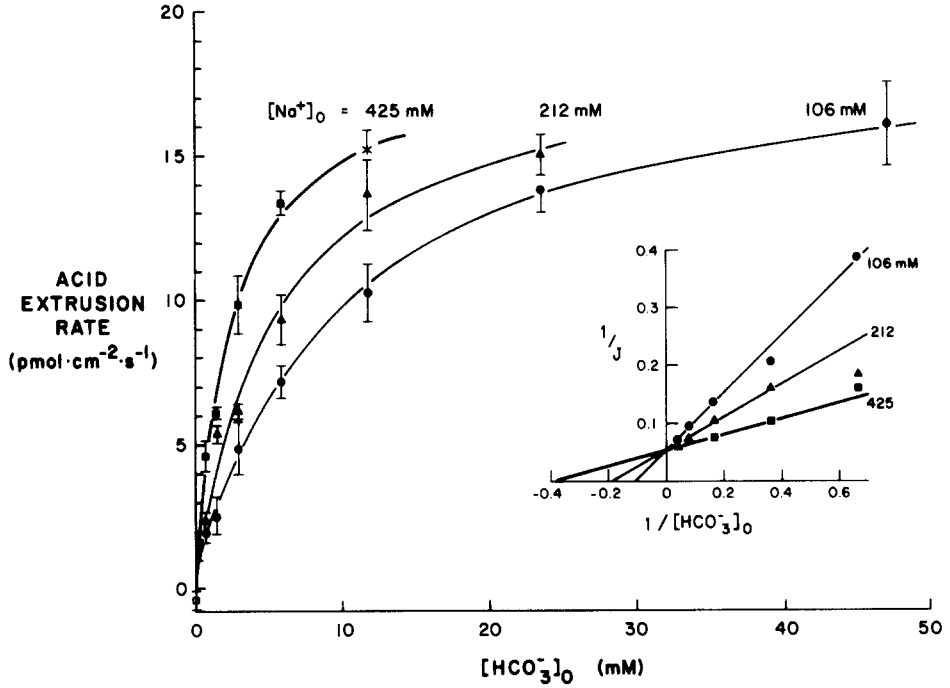

FIGURE 3. Dependence of acid extrusion rate (J_H) on $[HCO_3^-]_o$ at three fixed levels of $[Na^+]_o$: 425 (■), 212 (▲), and 106 mM (●). Data from experiments similar to that of Fig. 2 were fitted by nonlinear least-squares methods. The $[Na^+]_o$ = 425 mM curve (type 2 fit) was forced through the point corresponding to the composition of the standard solution (i.e., $[HCO_3^-]_o$ = 12 mM, indicated by the asterisk). The $[Na^+]_o$ = 212 and 106 mM curves represent type 1 fits to the standard Michaelis-Menten equation. The vertical bars indicate standard errors. In the inset, the data are replotted in double-reciprocal form. The straight lines through these replotted data are not the results of linear fits to a double-reciprocal transformation of the Michaelis-Menten equation. Instead, these lines are drawn according to the same K_m and J_{max} values used to construct the curved plots in the main part of the figure.

$[Na^+]_o$ = 425 mM, $[HCO_3^-]_o$ = 12 mM). The K_m (Na) was 71 ± 12 mM, which is not significantly different from the value of 77 ± 12 mM previously obtained on intact axons (Boron and Russell, 1983). Although the J_{max} obtained by varying $[Na^+]_o$ at 12 mM $[HCO_3^-]_o$ (i.e., 17.8 ± 3.0 pmol·cm^{-2}·s^{-1}) is not significantly different from that obtained by varying $[HCO_3^-]_o$ at 425 mM $[Na^+]_o$ (18.6 ± 1.2 pmol·cm^{-2}·s^{-1}), it exceeds that previously obtained in intact axons (i.e., 10.3 ±

TABLE I

Dependences of Acid Extrusion on $[HCO_3^-]_o$ at Three Levels of $[Na^+]_o$

$[Na^+]_o$	Fit*	n	Apparent K_m (HCO_3^-)	Apparent J_{max}
mM			*mM*	*pmol·cm^{-2}·s^{-1}*
425	2	31	2.6±0.3	18.6±1.2
212	1	40	5.4±1.0	18.7±1.2
106	1	44	9.7±2.1	19.2±1.5

* Type 1 fit: standard Michaelis-Menten equation. Type 2: the fit is forced through a standard point ($[HCO_3^-]_o$ = 12 mM, J_H = 15.3 pmol·cm^{-2}·s^{-1}). n is the number of points fitted.

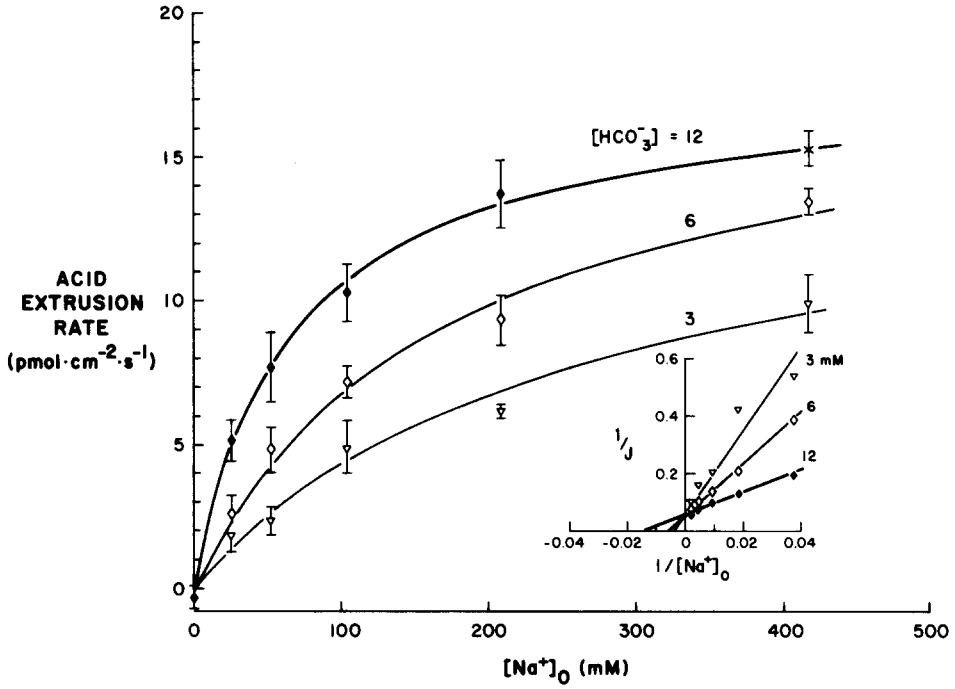

FIGURE 4. Dependence of acid extrusion rate (J_H) on $[Na^+]_o$ at three fixed levels of $[HCO_3^-]_o$: 12 (◆), 6 (◇), and 3 mM (▽). Data from experiments similar to that of Fig. 2 were fitted by nonlinear, least-squares methods. The curve for $[HCO_3^-]_o$ = 12 mM (type 2 fit) was forced through the point corresponding to the composition of the standard solution (i.e., $[Na^+]$ = 425 mM, indicated by the asterisk). The $[HCO_3^-]_o$ = 6 and 3 mM curves represent type 1 fits to the standard Michaelis-Menten equation. The vertical bars indicate standard errors. In the inset, the data are replotted in double-reciprocal form. The straight lines through these replotted data are drawn according to the same K_m and J_{max} values used to construct the curved plots in the main part of the figure.

0.6) by a considerable amount. As noted above, the discrepancy is probably due to the higher $[Cl^-]_i$ in the present study.

The data for $[HCO_3^-]_o$ values of 6 and 3 mM were first fitted to a standard Michaelis-Menten equation (type 1 fit). At an $[HCO_3^-]_o$ of 6 mM, the best-fit value for K_m (Na) was 174 ± 45 mM, 2.5-fold higher than that at 12 mM $[HCO_3^-]_o$ (see Table II, line 2, and Fig. 4, middle curve). J_{max}, on the other hand, was 18.4 ± 2.0 pmol·cm^{-2}·s^{-1}, which is not significantly different from the value in 12 mM $[HCO_3^-]_o$. Reducing $[HCO_3^-]_o$ to 3 mM, one-fourth of its control value, increased K_m (Na) ~3.7-fold, to 261 ± 102 mM (Table II, line 3, and Fig. 4, lower curve). Although J_{max} decreased somewhat, to 15.4 ± 3.2 mM, it was not significantly different from the value in 12 mM $[HCO_3^-]_o$. The accuracy of this last type 1 fit is expected to be limited, however, because the increase in K_m (Na) could not be matched by a corresponding increase in the maximal $[Na^+]_o$ tested in the experiments. I also fitted the 6 and 3 mM HCO_3^- data to a modified Michaelis-Menten equation in which J_{max} was predetermined (type 3 fit; see Methods). The chosen J_{max} was 18.6 pmol·cm^{-2}·s^{-1}, the value obtained by fitting

TABLE II

Dependences of Acid Extrusion on $[Na^+]_o$ at Three Levels of $[HCO_3^-]_o$

$[HCO_3^-]_o$	Fit*	n	Apparent K_m (Na^+)	Apparent J_{max}
mM			*mM*	*pmol·cm^{-2}·s^{-1}*
12	2	35	71±12	17.8±3.0
6	1	30	174±45	18.4±2.0
3	1	33	261±102	15.4±3.2
6	3	30	179±15	18.6
3	3	33	364±34	18.6

* Type 1 fit: standard Michaelis-Menten equation. Type 2: the fit is forced through a standard point. Type 3: J_{max} is preset to a lumped J_{max} value. n is the number of points fitted.

all the data of this study as a function of $[NaCO_3^-]_o$ (see below). This type 3 fit (Table II, line 5) resulted in approximately the same K_m values, but with substantially lower standard deviations. At 3 mM $[HCO_3^-]_o$, K_m (Na) was 364 ± 34 mM, ~5.1-fold greater than in 12 mM $[HCO_3^-]_o$. For the data in 6 mM $[HCO_3^-]_o$, the type 3 fit (Table II, line 4) yielded a K_m (Na) of 179 ± 15 mM, which is not very different from the value produced by the type 1 fit. In summary, the data of Table II are consistent with the $NaCO_3^-$ ion-pair model (see Discussion), which predicts that K_m (Na) should be inversely proportional to $[HCO_3^-]_o$, whereas J_{max} should be independent of $[HCO_3^-]_o$.

DISCUSSION

Validity of Approach

The kinetic analysis of the data is greatly simplified if the J_H values correspond to "initial" rates. One way this can be ensured in the present experiments is by removing internal Na^+, which obviates a possible reversal of the pH_i-regulating mechanism. Although dialysis with a Na-free solution should reduce $[Na^+]_i$ to

near-zero levels during the period of dialysis, $[Na^+]_i$ would be expected to rise after dialysis is halted. Although I have no data on Na^+ influxes under the present experimental conditions (pH_i = 6.6, $[Cl^-]_i$ = 400 mM), an influx of 10 pmol·cm^{-2}·s^{-1} would cause $[Na^+]_i$ to rise by <3 mM/h. A significant reversal of the pH_i-regulating mechanism is unlikely even at $[Na^+]_i$ levels exceeding 100

TABLE III

Summary of Data, Grouped by Calculated $[NaCO_3^-]_o$*

$[NaCO_3^-]_o$	$[Na^+]_o$	$[HCO_3^-]_o$	Acid extrusion rate	Mean pH_i	n
μM	*mM*	*mM*	*pmol·cm^{-2}·s^{-1}*		
402	425	12	15.3±0.6	6.69±0.01	63
	212	24	15.1±0.7	6.77±0.03	8
	106	48	16.1±1.5	6.73±0.03	6
201	425	6	13.4±0.4	6.85±0.03	7
	212	12	13.7±1.2	6.73±0.03	6
	106	24	13.9±0.8	6.69±0.01	6
100.5	425	3	9.9±1.0	6.74±0.05	6
	212	6	9.3±0.9	6.74±0.03	8
	106	12	10.3±1.0	6.71±0.02	10
50.3	425	1.5	6.2±0.2	6.83±0.02	6
	212	3	6.2±0.2	6.74±0.03	7
	106	6	7.2±0.6	6.76±0.04	4
	53	12	7.7±1.2	6.76±0.02	7
25.1	425	0.75	4.6±0.6	6.87±0.05	8
	212	1.5	5.4±0.3	6.78±0.06	4
	106	3	4.9±0.9	6.77±0.03	8
	53	6	4.9±0.8	6.79±0.05	5
	26.5	12	5.2±0.7	6.76±0.02	8
12.6	212	0.75	2.4±0.3	6.77±0.07	7
	106	1.5	2.6±0.7	6.81±0.05	5
	53	3	2.4±0.5	6.81±0.03	5
	26.5	6	2.6±0.7	6.74±0.03	6
6.3	106	0.75	2.0±0.3	6.72±0.05	5
	26.5	3	1.9±0.6	6.77±0.04	7
0.0	425	0	−0.4±0.4	6.95±0.04	4
	0	12	−0.3±0.4	6.72±0.06	4

* Within any group, the differences between calculated acid extrusion rates are not statistically significant, as determined by the unpaired Student's *t* test.

mM, given my inability to demonstrate such a reversal despite considerable effort (unpublished observations).

The acid extrusion rate of the squid axon is sensitive to changes in pH_i and $[Cl^-]_i$ (Boron and Russell, 1983). As can be seen in column 5 of Table III, the groups of data in the present study were obtained at rather similar mean pH_i

values. Furthermore, the pH_i dependence of J_H in squid axons apparently is not as great as in other cells. In barnacle muscle, for example, J_H is >10 times as great at pH_i 6.8 as at pH_i 7.3 (Boron et al., 1979), whereas in squid axons, this factor is only ~2 (Boron and Russell, 1983). Thus, the error introduced by pH_i variability should be minimal. The axon's pH_i-regulating mechanism has a K_m for internal Cl^- of ~84 mM (Boron and Russell, 1983). Because the nominal $[Cl^-]_i$ of 400 mM exceeded this by a factor of 4.7, it is unlikely that small shifts of $[Cl^-]_i$ during an experiment could have seriously affected J_H. In one control experiment, $[Na^+]_o$ and $[HCO_3^-]_o$ were kept approximately constant (at 425 mM and 12 mM, respectively), while I mimicked a normal sequence of solution changes. That is, four solutions were delivered from individual syringes, and pH_i was allowed to rise over its normal range. The values of J_H for the four solutions were indistinguishable, which confirmed my suspicion that small pH_i changes as well as possible variations in $[Cl^-]_i$ or $[Na^+]_i$ had a negligible effect on the results.

Kinetic Models of Acid Extrusion

The data of Figs. 3 and 4 can be analyzed in terms of several kinetic models. In the following discussion, I specifically consider the ion-pair hypothesis (Fig. 1 *D*) and the Na^+ plus $CO_3^=$ hypothesis (Fig. 1 *C*). The latter actually includes three kinetically distinct models: (*a*) the random binding of Na^+ and $CO_3^=$, (*b*) the ordered binding of Na^+ and then $CO_3^=$, and (*c*) the ordered binding of $CO_3^=$ and then Na^+. Because $[HCO_3^-]$ is proportional to $[CO_3^=]$ at constant pH, these three models dealing with Na^+ plus $CO_3^=$ (Fig. 1 *C*) apply equally well to models involving the binding of Na^+ plus a single HCO_3^- (Fig. 1 *A*). In addition, these three analyses could also apply to the binding of Na^+ and two HCO_3^- (Fig. 1 *B*), provided the binding of the two HCO_3^- is governed by sufficiently different equilibrium constants. Thus, the following discussion applies to models *A*, *C*, and *D* of Fig. 1, and may apply to model *B*.

THE $NaCO_3^-$ ION-PAIR MODEL The ion-pair hypothesis (Fig. 1 *D*) predicts that J_H should be determined by $[NaCO_3^-]_o$, which is proportional (at fixed pH_o) to the product $[Na^+]_o \cdot [HCO_3^-]_o$, and not by $[Na^+]_o$ or $[HCO_3^-]_o$ per se. The $NaCO_3^-$ model predicts the following values for apparent K_m (Na) and J_{max} (Na):

$$K_m\ (Na) = \frac{\gamma K_m [H^+]_o}{[HCO_3^-]_o}$$

and

$$J_{max}\ (Na) = J_{max},$$

where K_m is the true K_m for external $NaCO_3^-$, J_{max} is the true J_{max}, and $\gamma = ([Na^+] \cdot [HCO_3^-])/([NaCO_3^-] \cdot [H^+])$. Similarly, for the apparent K_m (HCO_3) and J_{max} (HCO_3) values:

$$K_m\ (HCO_3) = \frac{\gamma K_m [H^+]_o}{[Na^+]_o}$$

and

$$J_{max}\ (HCO_3) = J_{max}.$$

In other words, the apparent K_m values for Na^+ and HCO_3^- should be inversely proportional to the concentration of the opposite ion, and the J_{max} values should be independent of either $[Na^+]_o$ or $[HCO_3^-]_o$. Within experimental error, these predictions have been verified by the present data. Another expression of these kinetic predictions is that if the J_H data are plotted as a function of $[NaCO_3^-]_o$, they should all fall along the same Michaelis-Menten curve, regardless of the particular values of $[Na^+]_o$ or $[HCO_3^-]_o$ used to achieve the $[NaCO_3^-]_o$. Fig. 5 is a replot of all the J_H data of this study as a function of $[NaCO_3^-]_o$, the latter calculated from $[Na^+]_o$, $[HCO_3^-]_o$, and pH_o according to the stability constant

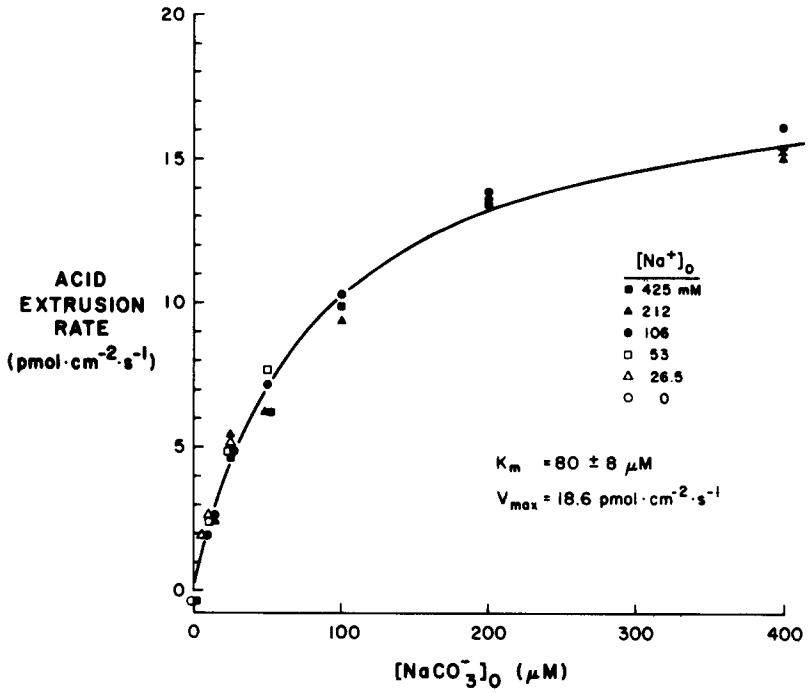

FIGURE 5. Dependence of acid extrusion rate on the calculated $[NaCO_3^-]_o$. The data from Figs. 3 and 4 are replotted as a function of $[NaCO_3^-]_o$, calculated from $[Na^+]_o$, $[HCO_3^-]_o$, and pH_o (pH_o = 8.0) according to the stability constant data of Garrels et al. (1961).

data of Garrels et al. (1961). It is clear that, within experimental error, all the data fall along the same Michaelis-Menten curve, which was drawn from best-fit values of 80 ± 8 μM for K_m ($NaCO_3^-$) and 18.6 ± 0.7 pmol·cm^{-2}·s^{-1} for J_{max}. These data are also presented in Table III, which shows that for any value of $[NaCO_3^-]_o$ there is no significant difference among J_H values obtained with different combinations of $[Na^+]_o$ and $[HCO_3^-]_o$. The present data are thus fully consistent with the ion-pair model.

RANDOM BINDING OF Na^+ AND $CO_3^=$ If Na^+ and $CO_3^=$ (Fig. 1 *C*) bind randomly to the transporters, and if the binding of each ion is rapid compared with the transport step, then the transport process can be described by the following

reaction sequence:

$$\begin{array}{ccc} X + \mathrm{Na} & \xrightleftharpoons{K_{\mathrm{Na}}} & X\cdot\mathrm{Na} \\ + & & + \\ \mathrm{CO_3} & & \mathrm{CO_3} \\ \Updownarrow K_c & & \Updownarrow \alpha K_c \\ X\cdot\mathrm{CO_3} + \mathrm{Na} & \xrightleftharpoons{\alpha K_{\mathrm{Na}}} & X\cdot\mathrm{Na}\cdot\mathrm{CO_3} \xrightarrow{k} \end{array}$$

where X is the transporter, K_{Na} and K_c are equilibrium constants, k is the rate constant of the slow transport step across the membrane, and α is the factor by which the equilibrium constant for the binding of one substrate is altered by the binding of the other substrate. Thus, when $\alpha = 1$, the affinity of the transporter for one substrate is unaffected by the binding of the other substrate, whereas if α falls below 1, the affinity is increased by the binding of the other substrate. The assumptions of rapid-equilibrium kinetics lead to the following predictions for the apparent J_{max} and the apparent K_m when $[Na^+]_o$ is varied at fixed $[CO_3^=]_o$ (i.e., at fixed pH_o and $[HCO_3^-]_o$):

$$K_m\ (\mathrm{Na}) = \frac{\alpha K_c + \alpha[CO_3^=]}{\alpha K_c + [CO_3^=]} K_{Na},$$

and

$$J_{max}\ (\mathrm{Na}) = \frac{[CO_3^=]}{[CO_3^=] + \alpha K_c} J_{max},$$

where J_{max} is the true maximal velocity for the reaction. Similarly, when $[CO_3^=]_o$ is varied at fixed $[Na^+]_o$:

$$K_m\ (CO_3) = \frac{\alpha K_{Na} + \alpha[Na^+]}{\alpha K_{Na} + [Na^+]} K_c,$$

and

$$J_{max}\ (CO_3) = \frac{[Na^+]}{[Na^+] + \alpha K_{Na}} J_{max}.$$

The kinetic predictions of this and several other models are given in Table IV, along with the experimental observations. To minimize the bias, only the results of type 1 and type 2 fits are included in Table IV. Inasmuch as $[HCO_3^-]$ is proportional to $[CO_3^=]$ at constant pH, I will refer to HCO_3^- as the independent variable. The K_m (HCO_3^-) and J_{max} (HCO_3^-) values at 212 and 106 mM Na^+ are given relative to the values in 425 mM Na^+ (assumed to be unity). Conversely, K_m (Na^+) and J_{max} (Na^+) values at 6 and 3 mM HCO_3^- are given relative to the values at 12 mM HCO_3^-. The predicted values that fall >2 SD from the observed value are given in parentheses. The predictions of the rapid-equilibrium, random-binding model depend on the value chosen for α. For an α of unity (Table IV, line 1), the predicted K_m values are independent of the concentration of the

alternative substrate, whereas the predicted J_{max} values vary by modest amounts. The predicted invariability of the K_m values is clearly at odds with the data (compare lines 1 and 8). Even the predicted, modest changes in J_{max} (HCO_3) are >2 SD away from the negligible changes observed. Although the predicted J_{max} (Na) values are within 2 SD of the observed ones, this is probably the fortuitous consequence of the large standard deviations of the curve-fitted (i.e., experimental) values.[1]

If the assumed α is lowered to 0.5 or to 0.1, the predicted K_m and J_{max} values still fall >2 SD from the observed values, although the discrepancy is smaller. If α is zero, however, the kinetic predictions of the random-binding model are exactly the same as those of the ion-pair model. I therefore cannot rule out a rapid-equilibrium, random-binding model[2] if α is sufficiently close to zero. An α of zero implies that once the transporter binds one substrate, it has an infinite

TABLE IV

Predictions of Rapid-Equilibrium Kinetic Models

	K_m (Na)			J_{max} (Na)			K_m (HCO_3)			J_{max} (HCO_3)		
	$[HCO_3^-]_o$, mM			$[HCO_3^-]_o$, mM			$[Na^+]_o$, mM			$[Na^+]_o$, mM		
	12	6	3	12	6	3	425	212	106	425	212	106
(1) Random Na^+ and $CO_3^=$, $\alpha = 1$	1.00	(1.00)	(1.00)	1.00	0.85	0.66	1.00	(1.00)	(1.00)	1.00	(0.87)	(0.70)
(2) Random Na^+ and $CO_3^=$, $\alpha = 0.5$	1.00	(1.07)	(1.19)	1.00	0.91	0.78	1.00	(1.06)	(1.16)	1.00	(0.93)	(0.81)
(3) Random Na^+ and $CO_3^=$, $\alpha = 0.1$	1.00	(1.15)	(1.44)	1.00	0.97	0.94	1.00	(1.12)	(1.36)	1.00	(0.98)	(0.95)
(4) Random Na^+ and $CO_3^=$, $\alpha = 0$	1.00	2.00	4.00	1.00	1.00	1.00	1.00	2.00	4.00	1.00	1.00	1.00
(5) Ordered, Na^+ then $CO_3^=$	1.00	1.70	2.61	1.00	0.85	0.65	1.00	(1.14)	(1.44)	1.00	1.00	1.00
(6) Ordered, $CO_3^=$ then Na^+	1.00	(1.18)	(1.53)	1.00	1.00	1.00	1.00	1.75	2.80	1.00	(0.87)	(0.70)
(7) $NaCO_3^-$	1.00	2.00	4.00	1.00	1.00	1.00	1.00	2.00	4.00	1.00	1.00	1.00
(8) Observed	1.00	2.45 ±0.63	3.68 ±1.44	1.00	1.03 ±0.11	0.87 ±0.18	1.00	2.08 ±0.39	3.73 ±0.81	1.00	1.01 ±0.06	1.03 ±0.08

affinity for (i.e., automatically binds) the other substrate. Thus, for all practical purposes, the case in which α approaches zero is kinetically indistinguishable from the ion-pair model. It is theoretically distinct, however, inasmuch as the binding of Na^+ and $CO_3^=$ to separate sites would be quite different mechanistically from the binding of a $NaCO_3^-$ to a single site.

If the binding of Na^+ and $CO_3^=$ (or HCO_3^-) is not rapid compared with the transport step, the assumptions of rapid-equilibrium kinetics are not valid, and

[1] The observed (i.e., fitted) values for K_m (Na) and J_{max} (Na) have anomalously high standard deviations for $[HCO_3^-]_o$ = 6 mM, and especially for $[HCO_3^-]_o$ = 3 mM. These parameters, the result of type 1 curve fits, can be determined only with limited accuracy when $[Na^+]_o$ cannot be raised sufficiently to have J approach J_{max}.

[2] Because $[HCO_3^-]$ is proportional to $[CO_3^=]$ at constant pH, the predictions of any model for the binding of Na^+ and one HCO_3^- are the same as those for Na^+ and $CO_3^=$.

the data must be analyzed by the much more complex "steady state" approach (Segal, 1975). Although I have not attempted such an analysis, there are two reasons why it is likely that a set of rate constants could be found for which a steady state, random-binding model could account for the data. First, the rapid-equilibrium approach can account for the data as α approaches zero, and the steady state approach is even more general. Second, as noted below, the two ordered-binding, steady state models can account for the data, and the random-binding model is even more general.

ORDERED BINDING OF Na^+ AND $CO_3^=$ If Na^+ and then $CO_3^=$ (Fig. 1*C*) bind to the transporter, and if these binding steps are rapid compared with the transport step, the overall transport process can be described by the following reaction sequence:

$$\begin{array}{ccc} X + \mathrm{Na} & \overset{K_{\mathrm{Na}}}{\rightleftharpoons} & X\cdot\mathrm{Na} \\ & & + \\ & & \mathrm{CO_3} \\ & & \uparrow\downarrow K_c \\ & & X\cdot\mathrm{Na}\cdot\mathrm{CO_3} \xrightarrow{k} \end{array}$$

The assumptions of rapid-equilibrium kinetics lead to the following predictions for the apparent K_m and J_{max} values:

$$K_m\ (\mathrm{Na}) = \frac{K_c}{K_c + [\mathrm{CO_3^=}]} K_{\mathrm{Na}},$$

$$J_{max}\ (\mathrm{Na}) = \frac{[\mathrm{CO_3^=}]}{K_c + [\mathrm{CO_3^=}]} J_{max},$$

and

$$K_m\ (\mathrm{CO_3}) = \frac{[\mathrm{Na^+}] + K_{\mathrm{Na}}}{[\mathrm{Na^+}]} K_c,$$

$$J_{max}\ (\mathrm{CO_3}) = J_{max}.$$

The predicted K_m and J_{max} values for this model are given in Table IV, line 5. The predicted J_{max} values,[1] as well as the K_m (Na) values, are within 2 SD of the observations. However, the predicted values of K_m (HCO_3) are substantially less than those observed, allowing us to rule out the rapid-equilibrium, ordered binding of Na^+ then $CO_3^=$ (or HCO_3^-) for the squid axons.[2]

If the binding of Na^+ and $CO_3^=$ (or HCO_3^-) is not rapid compared with the transport step, then the more general approach of steady state kinetics must be applied. Sanders et al. (1984) have analyzed the kinetic predictions of an ordered-binding cotransport model for a variety of boundary conditions. Their analysis of the "zero trans-ligand" boundary condition (analogous to $[Na^+]_i = 0$ in my experiments) shows that for a restricted combination of rate constants (see their Table II, column 2, rows 9 and 10), the ordered binding of Na^+ and $CO_3^=$ (or

HCO_3^-) can account for my data. The reverse order of binding (i.e., $CO_3^=$ or HCO_3^-, then Na^+) can also account for my data, given a similarly restricted combination of rate constants.

ORDERED BINDING OF $CO_3^=$ AND Na^+ If $CO_3^=$ and then Na^+ (Fig. 1*C*) bind to the transporter, and if these binding steps are rapid compared with the transport step, the overall transport process can be described by the following reaction sequence:

$$\begin{array}{l} X + CO_3 \overset{K_c}{\rightleftharpoons} X \cdot CO_3 \\ \qquad\qquad\quad + \\ \qquad\qquad\quad Na \\ \qquad\qquad\quad \Updownarrow K_{Na} \\ \qquad\qquad\quad X \cdot Na \cdot CO_3 \xrightarrow{k} \end{array}$$

The assumptions of rapid-equilibrium kinetics lead to the following predictions for apparent K_m and J_{max} values:

$$K_m\ (Na) = \frac{[CO_3^=] + K_c}{[CO_3^=]} K_{Na},$$

$$J_{max}\ (Na) = J_{max},$$

$$K_m\ (CO_3) = \frac{K_{Na}}{K_{Na} + [Na^+]} K_c,$$

and

$$J_{max}\ (CO_3) = \frac{[Na^+]}{K_{Na} + [Na^+]} J_{max}.$$

The pattern of predicted K_m and J_{max} values (listed in Table IV, line 6) is the opposite of that for the ordered binding of Na^+ and then $CO_3^=$. The predicted changes in J_{max} (Na) agree with the data. However, all other predicted kinetic parameters deviate >2 SD from the observations. Thus, the rapid-equilibrium, ordered binding of $CO_3^=$ (or HCO_3^-) and then Na^+ is ruled out as a possible explanation for acid extrusion in the squid axon.[2] However, the assumptions of rapid-equilibrium kinetics place restrictions on the ordered-binding model. As noted above, the more general approach of steady state kinetics can account for the present data, but only for a constrained set of rate constants.

In summary, the present data are entirely consistent with the predictions of the ion-pair model. Although other general models cannot be ruled out, they can account for the data only under severely restricted conditions. That is, rapid-equilibrium models for the ordered binding of Na^+ and then $CO_3^=$ (or vice versa) are ruled out, as are rapid-equilibrium models for the random binding of these ions unless the factor α approaches zero. The comparable steady state kinetic models do account for the data, but only for limited combinations of rate constants.

Comparison with the pH_i-regulating System of Barnacle Muscle

As noted in the Introduction, a similar though less complete kinetic study of the pH_i-regulating system in the barnacle muscle fiber (Boron et al., 1981) yielded data inconsistent with the ion-pair model. Specifically, when the $[Na^+]_o$ dependence was examined at two different $[HCO_3^-]_o$ values (at a constant pH_o of 8.0), there were only slight effects on K_m (Na), but there was a substantial change in J_{max} (Na). This is the opposite of the pattern observed in the present experiments and the opposite of that predicted by the ion-pair model. More recently, A. Roos and T. J. Wilding (unpublished observations) have studied the $[HCO_3^-]_o$ dependence of acid extrusion at external Na^+ concentrations of 440 and 40 mM in barnacle muscle. They found that altering $[Na^+]_o$ has a major effect on J_{max} (HCO_3), and only small effects on K_m (HCO_3). These results are compatible with those previously obtained on barnacle muscle (Boron et al., 1981), and again indicate that the ion-pair hypothesis cannot account for pH_i regulation in that preparation. It thus appears that there is a consistent difference between the kinetics of the pH_i regulator in barnacle muscle and squid axons: the barnacle data are consistently irreconcilable with the ion-pair model, whereas the squid data are consistently supportive of this model. These kinetic differences are not the first discrepancies between the pH_i regulators of these two preparations. The barnacle muscle's transporter is easily reversible (Russell et al., 1983), is stimulated by cyclic AMP (Boron et al., 1978), and is supported by Li^+ nearly as well as by Na^+ (Boron et al., 1981). The squid axon's transporter, on the other hand, has not been reversed despite considerable effort (unpublished observations), is not stimulated by cyclic AMP (Russell, J. M., and W. F. Boron, unpublished observations), and is not supported by Li^+ (Boron and Russell, 1983). Thus, although the pH_i-regulating systems superficially appear similar in squid axons and barnacle muscle, there are several more subtle differences between them.

I thank J. M. Russell for his comments on an earlier draft of this paper, and for allowing me to borrow one of the two dialysis assemblies used in these experiments. In addition, I am grateful to C. L. Slayman for helpful discussions on steady state kinetics, P. Fong for her tireless assistance in the execution of these experiments, and A. Yeatts for the design and manufacture of the solution-changing device and its computer interface.

This work was funded by a grant from the National Institutes of Health (RO1 NS18400). The author is supported by a Research Career Development Award (KO4 AM01022).

Original version received 22 June 1984 and accepted version received 22 October 1984.

REFERENCES

Becker, B. F., and J. Duhm. 1978. Evidence for anionic cation transport of lithium, sodium and potassium across the human erythrocyte membrane induced by divalent anions. *J. Physiol. (Lond.).* 282:149–168.

Boron, W. F., and P. De Weer. 1976. Intracellular pH-transients in squid giant axons caused by CO_2, NH_3, and metabolic inhibitors. *J. Gen. Physiol.* 67:91–112.

Boron, W. F., W. C. McCormick, and A. Roos. 1979. pH regulation in barnacle muscle fibers: dependence on intracellular and extracellular pH. *Am. J. Physiol.* 237:C185–C193.

Boron, W. F., W. C. McCormick, and A. Roos. 1981. pH regulation in barnacle muscle fibers: dependence on extracellular sodium and bicarbonate. *Am. J. Physiol.* 240:C80–C89.

Boron, W. F., and J. M. Russell. 1983. Stoichiometry and ion dependencies of the intracellular pH-regulating mechanism in squid giant axons. *J. Gen. Physiol.* 81:373–399.

Boron, W. F., J. M. Russell, M. S. Brodwick, D. W. Keifer, and A. Roos. 1978. Influence of cyclic AMP on intracellular pH regulation and chloride fluxes in barnacle muscle fibers. *Nature (Lond.).* 276:511–513.

Brinley, F. J., Jr., and L. J. Mullins. 1965. Variations in the chloride content of isolated squid axons. *Physiologist.* 8:121.

Brinley, F. J., Jr., and L. J. Mullins. 1967. Sodium extrusion by internally dialyzed squid axons. *J. Gen. Physiol.* 50:2303–2311.

Garrels, R. M., M. E. Thompson, and R. Siever. 1961. Control of carbonate solubility by carbonate complexes. *Am. J. Sci.* 259:24–45.

Hinke, J. A. M. 1967. Cation-selective microelectrodes for intracellular use. *In* Glass Electrodes for Hydrogen and Other Cations. G. Eisenman, editor. Marcel Dekker, New York. 464–477.

Moody, W. J., Jr. 1981. The ionic mechanism of intracellular pH regulation in crayfish neurones. *J. Physiol. (Lond.).* 316:293–308.

Roos, A., and W. F. Boron. 1981. Intracellular pH. *Physiol. Rev.* 61:296–434.

Russell, J. M. 1976. ATP-dependent chloride influx into internally dialyzed squid giant axons. *J. Membr. Biol.* 28:335–349.

Russell, J. M., and W. F. Boron. 1976. Role of chloride transport in regulation of intracellular pH. *Nature (Lond.).* 264:73–74.

Russell, J. M., W. F. Boron, and M. S. Brodwick. 1983. Intracellular pH and Na fluxes in barnacle muscle with evidence for reversal of the ionic mechanism of intracellular pH regulation. *J. Gen. Physiol.* 82:47–78.

Sanders, D., U. P. Hansen, D. Gradmann, and C. L. Slayman. 1984. Generalized kinetic analysis of ion-driven cotransport systems: a unified interpretation of selective ionic effects on Michaelis parameters. *J. Membr. Biol.* 77:123–152.

Scarborough, J. B. 1966. Numerical Mathematical Analysis. Johns Hopkins University Press, Baltimore, MD. 600 pp.

Segal, I. H. 1975. Enzyme Kinetics. John Wiley & Sons, New York. 957 pp.

Thomas, R. C. 1977. The role of bicarbonate, chloride and sodium ions in the regulation of intracellular pH in snail neurones. *J. Physiol. (Lond.).* 273:317–338.